Original Paper _____ *Forma*, **11**, 1–25, 1996

Biological Invasion of an Organism with Separate Mobile and Stationary States: Modeling and Analysis

M. A. LEWIS and G. SCHMITZ

Department of Mathematics, University of Utah, JWB 233, Salt Lake City, UT 84112, U.S.A.

(Received October 30, 1995; Accepted December 20, 1995)

Keywords: Biological Invasion, Wave, Mobile, Stationary, Switching

Abstract. We model a biological invasion with separate mobile and stationary states for dispersal and reproduction. Transfer terms permit organisms to switch states. Formulating the problem as a nonlinear parabolic system, we analyse traveling wave solutions and calculate the invasion speed. Results show that even when transfer rates are infinitesimally small, a rapid invasion can occur.

1. Biological Background

Whereas classical partial differential equation models for biological invasions assume that populations grow and disperse continually (MURRAY, 1989), biological reality may be far different. For example, many populations, ranging from plants to birds, reproduce and disperse at separate distinct times in the year, and thus are understood far better using models such as integro-difference equations (KOT, 1992; VEIT and LEWIS, 1995). Even when populations do not have distinct reproductive and dispersive seasons, it is rare that these two events actually occur simultaneously. It is far more likely that individuals switch between a sessile reproductive state and a mobile state with no reproduction. In this paper we investigate the effect that this life history dynamic has on the spread rate for biological invasion.

Our original impetus for studying this problem came from modeling microbes spreading into a new environment (LEWIS *et al.*, 1995). In their stationary state microbes are bound to plants, and in their mobile state they move in the air or in the ground water. While stationary microbes are able to reproduce, they cannot spread into the new environment. On the other hand, mobile microbes are able to spread into uncolonized regions and access new resources, yet they typically do not reproduce until they switch back to the stationary state. Individuals in the mobile state have the added cost of a high mortality rate. It became clear to us that this life history dynamic is found in a wide variety of organisms, being typical for species not meeting the stringent modeling requirement

found in the classical partial differential equation models of simultaneous reproduction and movement.

In this paper we formulate our model under the following assumptions about the organism's life history:

1. Individuals switch from mobile to stationary state according to a Poisson process with rate λ_{ms}.
2. Individuals switch from stationary to mobile state according to a Poisson process with rate λ_{sm}.
3. Individuals in the stationary state undergo logistic growth.
4. Individuals in the mobile state undergo density-independent mortality according to a Poisson process with rate μ.
5. Individuals in the mobile state move according to a simple random walk process.

Our purpose in this paper is to calculate analytically the rate at which an organism, newly introduced into a region, will spread spatially. This model can be considered a natural extension of the classic Fisher equation (FISHER, 1937) accounting for mobile and stationary states in an individual's life.

2. The Model

The relevant equations, incorporating the assumptions given in the previous section, are:

$$\left.\begin{aligned} \frac{\partial s}{\partial t} &= rs\left(1-\frac{s}{k}\right)+\lambda_{ms}m-\lambda_{sm}s \\ \frac{\partial m}{\partial t} &= -\mu m-\lambda_{ms}m+\lambda_{sm}s+D\frac{\partial^2 m}{\partial x^2} \end{aligned}\right\}, \tag{1}$$

where $s(x,t)$ is the density of organisms in the stationary state and $m(x,t)$ is the density of organisms in the mobile state, x being space and t being time; λ_{sm} is the rate of switching from stationary to mobile state and λ_{ms} is the rate of switching from a mobile to stationary state; r is the intrinsic rate of reproduction in the stationary class and k is the carrying capacity; μ is the density-independent mortality rate in the mobile state and D is the diffusion coefficient describing the random motion. It is assumed, unless otherwise indicated, that the parameters λ_{ms}, λ_{sm}, and μ are positive and that the rate of reproduction in the stationary class exceeds the transfer rate from stationary to mobile classes, so that $r > \lambda_{sm}$.

To focus on hey parameters and to facilitate analysis we nondimensionalize the model (1) by defining the new variables

$$s^* = \frac{s}{k}, \quad m^* = \frac{m}{k}, \quad t^* = rt, \quad x^* = \frac{x}{\sqrt{Dr}},$$
$$\lambda_{ms}^* \frac{\lambda_{ms}}{r}, \quad \lambda_{sm}^* \frac{\lambda_{sm}}{r}, \quad \mu^* = \frac{\mu}{r}.$$

Dropping the asterisks for notational simplicity, we have

$$\left.\begin{aligned} \frac{\partial s}{\partial t} &= s(1-s) + \lambda_{ms} m - \lambda_{sm} s = f(s,m) \\ \frac{\partial m}{\partial t} &= -\mu m - \lambda_{ms} m + \lambda_{sm} s + \frac{\partial^2 m}{\partial x^2} = g(s,m) + \frac{\partial^2 m}{\partial x^2} \end{aligned}\right\}. \tag{2}$$

Null clines for the spatially homogeneous version of (2), satisfying $f = 0$ and $g = 0$, respectively, are:

$$m = \frac{1}{\lambda_{ms}}\left(\lambda_{sm} s - s(1-s)\right) \tag{3}$$

$$s = \frac{\mu + \lambda_{ms}}{\lambda_{sm}} m. \tag{4}$$

Solving (3) and (4) simultaneously yields the trivial equilibrium and a positive equilibrium, $(\bar{s}, \bar{m})$, where

$$\bar{s} = 1 - \lambda_{sm}\left(1 - \frac{\lambda_{ms}}{\mu + \lambda_{ms}}\right) \tag{5}$$

$$\bar{m} = \frac{\lambda_{sm}}{\mu + \lambda_{ms}} \bar{s}. \tag{6}$$

3. A Wave of Invasion

A wave of invasion by organisms from both the mobile and stationary pools is shown by a traveling wave solution moving at a constant speed, c, and with a constant profile. Mathematically, these requirements are captured in a change of variables:

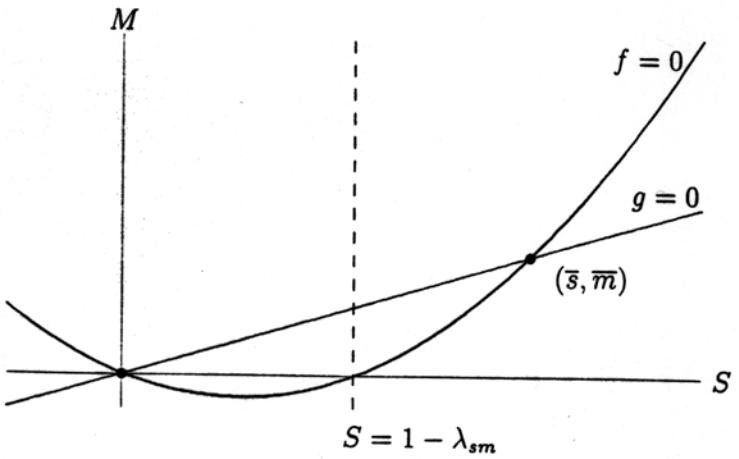

Fig. 1. Nullclines of the spatially independent version of Eq. (4).

$$(s,m)(x,t) = (S,M)(x-ct) = (S,M)(z), \tag{7}$$

where $z = x - ct$. This describes a solution moving with velocity c in the positive x direction. In the new coordinate, the system of partial differential Eq. (2) becomes

$$\left.\begin{aligned} -cS' &= -S^2 + S(1-\lambda_{sm}) + \lambda_{ms}M = f(S,M) \\ -cM' &= -\mu M - \lambda_{ms}M + \lambda_{sm}S + M'' = g(S,M) + M'' \end{aligned}\right\}, \tag{8}$$

where prime denotes differentiation with respect to z. Because s and m represent population densities, we seek traveling wave solutions $S(z) \geq 0$ and $M(z) \geq 0$ for all z.

Defining $\Theta = M'$, a wave of invasion is given by the boundary conditions:

$$\left.\begin{aligned} S(-\infty) &= \bar{s}, & M(-\infty) &= \bar{m}, & \Theta(-\infty) &= 0, \\ S(\infty) &= 0, & M(\infty) &= 0, & \Theta(\infty) &= 0. \end{aligned}\right\} \tag{9}$$

These boundary conditions imply that c must be positive. To see this, it is helpful to look at the null clines of the spatially independent version of (8), shown in Fig. 1. If M is non-negative then $c \neq 0$, because $c = 0$ would imply $f(S,M) = 0$, and the solution for (8) satisfying (9) would thus have a trajectory lying exactly on the null cline $f = 0$. However, on this null cline $M < 0$ for $S < 1 - \lambda_{sm}$, a contradiction.

Not only must $c \neq 0$, but $c > 0$, as we show here. A trajectory satisfying the boundary conditions (9) must cross the line $S = 1 - \lambda_{sm}$ at least once with $S' \leq 0$. First we eliminate the case where $S = 1 - \lambda_{sm}$ and $S' = 0$. Here the trajectory is again on $f = 0$ and so $M = 0$,

and either (i) $M' \neq 0$ or (ii) $M' = 0$ and $M'' < 0$ by (8). In either of these cases $M < 0$ in some neighborhood of $(S,M) = (1 - \lambda_{sm}, 0)$, contradicting our assumption of non-negativity. This means that a trajectory must cross $S = 1 - \lambda_{sm}$ with S' strictly less than zero. Then. for some z, $S = 1 - \lambda_{sm}$ and $S' < 0$, and we have in the first equation of system (8)

$$\begin{aligned} -cS' &= -\left(1-\lambda_{sm}\right)^2 + \left(1-\lambda_{sm}\right)^2 + \lambda_{ms}M \\ &= \lambda_{ms}M \geq 0, \end{aligned} \tag{10}$$

which implies that $c \geq 0$. We excluded the case $c = 0$ in the previous paragraph and thus c must be positive.

4. Local Stability

The eigenvalues associated with linearization about the trivial equilibrium are given by the roots of

$$P_0(\sigma) = \sigma^3 + A_1\sigma^2 + A_2\sigma + A_3 \tag{11}$$

where

$$A_1 = \frac{1 - \lambda_{sm} + c^2}{c} \tag{12}$$

$$A_2 = 1 - \lambda_{sm} - \left(\mu + \lambda_{ms}\right) \tag{13}$$

$$A_3 = \frac{-\left(\lambda_{ms}\lambda_{sm} + \left(1-\lambda_{sm}\right)\left(\mu + \lambda_{ms}\right)\right)}{c}. \tag{14}$$

According to Descartes' rule of signs, $P_0(\sigma)$ has one positive root. The other two roots have negative real parts, thus indicating that (0,0,0) is hyperbolic, with a stable two-dimensional subspace and an unstable one-dimensional subspace; these are tangent respectively to the corresponding linear stable and unstable subspaces at the origin (GUCKENHEIMER and HOLMES, 1983; AMANN, 1990).

The characteristic equation associated with the nontrivial steady state is

$$P_1(\sigma) = \sigma^3 + B_1\sigma^2 + B_2\sigma + B_3, \tag{15}$$

where

$$B_1 = \frac{\left(-2\bar{s}+1-\lambda_{sm}\right)+c^2}{c} \tag{16}$$

$$B_2 = \left(-2\bar{s}+1-\lambda_{sm}\right)-\left(\mu+\lambda_{ms}\right) \tag{17}$$

$$B_3 = -\frac{\lambda_{ms}\lambda_{sm}+\left(\mu+\lambda_{ms}\right)\left(-2\bar{s}+1-\lambda_{sm}\right)}{c}. \tag{18}$$

Noting that

$$-2\bar{s}+1-\lambda_{sm} = -\bar{s}-\frac{\lambda_{ms}\lambda_{sm}}{\mu+\lambda_{ms}} < 0 \tag{19}$$

and applying Descartes' rule of signs shows $P_1(\sigma)$ has one negative root. The other two roots have positive real parts, indicating that $(\bar{s},\bar{m},0)$ is also hyperbolic, with a one-dimensional stable manifold and a two-dimensional unstable manifold; these are tangent respectively to the stable and unstable subspaces of the linearized system at $(\bar{s},\bar{m},0)$.

In Section 5 we give numerical evidence of the existence of a heteroclinic orbit satisfying (9) via a shooting method. Here a starting point in a neighborhood of $(\bar{s},\bar{m},0)$ is specified to be on the span of the two unstable eigenvectors associated with $(\bar{s},\bar{m},0)$ and is parameterized by a single variable. Similarly, an ending point, in a neighborhood of (0,0,0) is specified to be on the span of the two stable eigenvectors associated with (0,0,0) and is parameterized by a single variable. Then the shooting method, with a variable length of integration, as given by (FRIEDMAN and DOEDEL, 1991), is used to find a solution connecting the two points.

5. Wave Speed Results

In this section we determine biologically valid wave speeds for the traveling wave system (8), (9). Our key argument is based upon the exclusion of wave speeds that do not satisfy the non-negativity requirement. The wave speed c at which the eigenvalues associated with the leading edge of the wave switch from real to complex, as in Fig. 2(b), are given by $P_0(\sigma) = P_0'(\sigma) = 0$. Using Sylvester's Dialytic Method of Elimination yields

$$4A_3A_1^4 - 18A_1^2A_2A_3 + 27A_1A_3^2 + 4A_1A_2^3 - A_1^3A_2^2 = 0 \tag{20}$$

and the application of (12)–(14), gives (20) as:

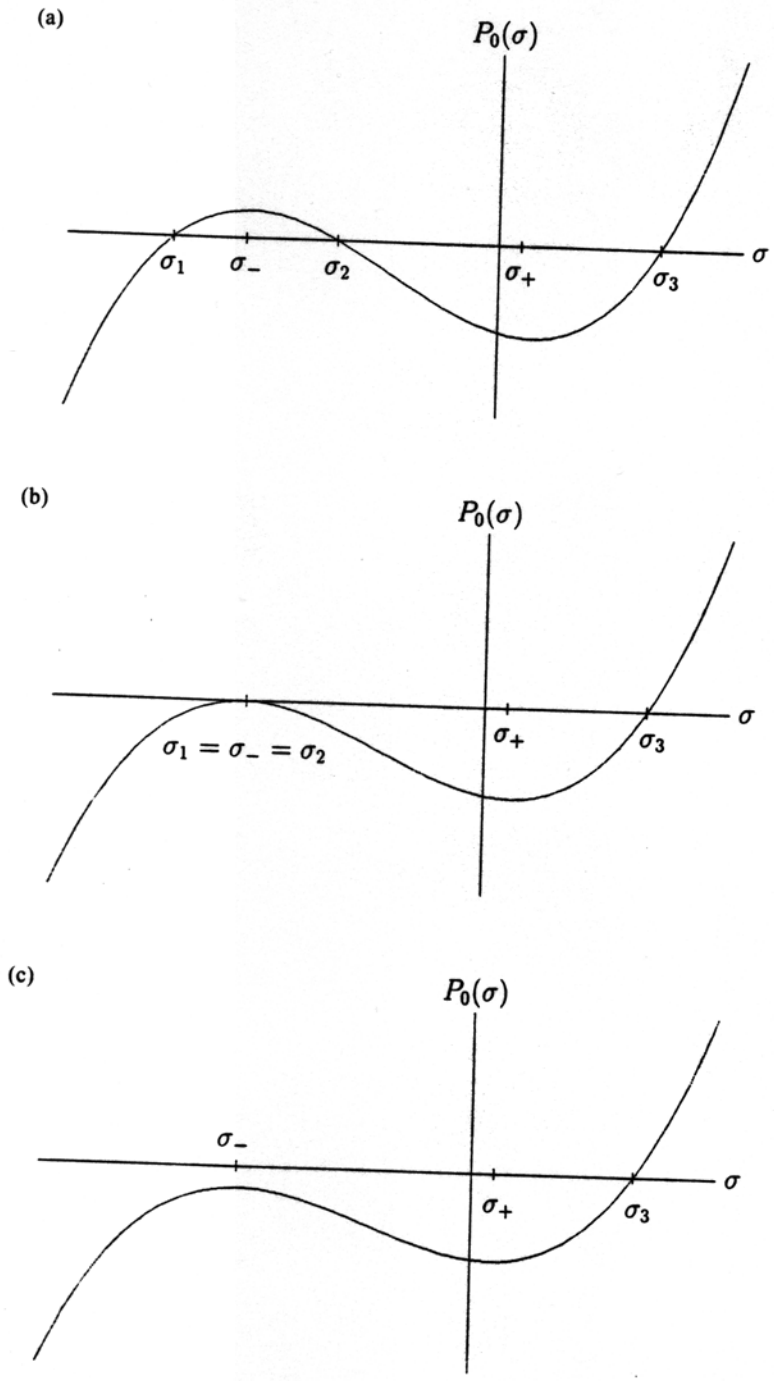

Fig. 2. Roots for the polynomial $P_0(\sigma)$ in Eq. (17). Each graph has the single positive real root σ_3. In addition there are: (a) two distinct negative roots; (b) two repeated negative roots; (c) two complex roots with negative real part.

$$\frac{\left(k_2 + c^2\right)}{c^5}\left(D_3 c^6 + D_2 c^4 + D_1 c^2 + D_0\right) = 0 \tag{21}$$

where

$$D_3 = -4\left(\lambda_{sm}\lambda_{ms} + k_1 k_2\right) - \left(k_2 - k_1\right)^2$$

$$D_2 = 6\left(\lambda_{sm}\lambda_{ms} + k_1 k_2\right)\left(k_2 - 3k_1\right) + 2\left(k_2 - k_1\right)^2\left(k_2 - 2k_1\right)$$

$$D_1 = 6k_2\left(\lambda_{sm}\lambda_{ms} + k_1 k_2\right)\left(k_2 - 3k_1\right) - k_2^2\left(k_2 - k_1\right)^2 + 27\left(\lambda_{sm}\lambda_{ms} + k_1 k_2\right)^2$$

$$D_0 = -4\left(\lambda_{sm}\lambda_{ms} + k_1 k_2\right)k_2^3$$

and

$$k_1 = \left(\mu + \lambda_{ms}\right) \tag{22}$$

$$k_2 = \left(1 - \lambda_{sm}\right). \tag{23}$$

When Eq. (21) holds, the graph of $P_0(\sigma)$ will qualitatively be like Fig. 2(b). The essential roots of (21) are contained in the following cubic in c^2:

$$R\left(c^2\right) = D_3 c^6 + D_2 c^4 + D_1 c^2 + D_0 = 0. \tag{24}$$

It can be shown numerically that two distinct positive roots for c^2 in (24), occur over the biologically reasonable range:

$$\left.\begin{aligned} 0 < \mu < 100 \\ 0 < \lambda_{ms} < 100 \\ 0 < \lambda_{sm} < 1 \end{aligned}\right\}. \tag{25}$$

Here λ_{sm} was chosen to satisfy our assumption that the intrinsic rate of reproduction in the stationary state exceeds the transfer rate from stationary to mobile classes.

Accordingly, we take square roots of the two positive solutions to (24) in c^2, giving us two critical, positive values of c. These values. $0 < c_1 < c_2$ result in a graph of $P_0(\sigma)$ that

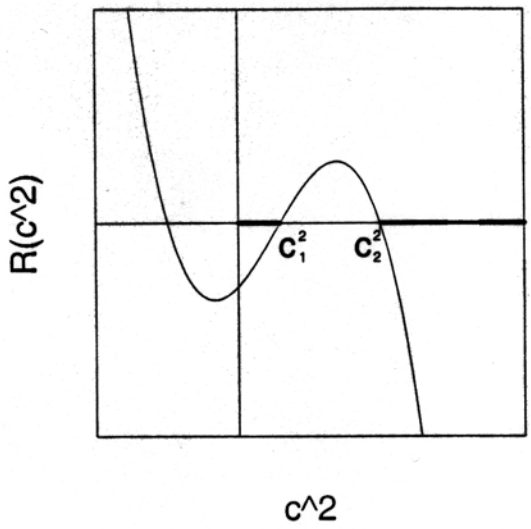

Fig. 3. Ranges of valid values for c, with $c_1{}^2$ and $c_2{}^2$ given as the positive roots to (33).

looks qualitatively like Fig. 2(b). For the remainder of the paper, we will assume that we have exactly two real positive roots of (24). These two positive roots introduce two ranges of valid values for c, $(0,c_1]$ and $[c_2,\infty)$, as in Fig. 3.

The local maximum of $P_0(\sigma)$ for a wave speed c is given by:

$$F(c) = P_0\big(\sigma_0(c)\big) = \sigma_0^3 + A_1\sigma_0^2 + A_2\sigma_0 + A_3, \tag{26}$$

where σ_0 solves

$$0 = P_0{}'(\sigma) = 3\sigma^2 + 2A_1\sigma + A_2. \tag{27}$$

A combination of analytical and numerical arguments can be used to show that $F(c)$ is positive on $(0,c_1)$ and (c_2,∞), is negative on (c_1,c_2) and satisfies a transversality condition $dF/dc \neq 0$ for $c = c_1, c_2$ (SCHMITZ, 1993). In other words, whereas orbits do spiral towards the origin for $c \in (c_1,c_2)$, they do not spiral towards the origin for the two ranges of valid values of c: $(0,c_1]$ and $[c_2,\infty)$.

These results are confirmed by solving (8) numerically, using the method described at the end of Section 4. Figure 4 depicts a solution, shown in the S-M plane, with $c > c_2$. Notice that the solution stays positive. For $c \in (c_1,c_2)$, the solution spirals to the origin, going negative in S and M as depicted in Fig. 5.

Though there are two ranges of wave speeds for which waves do not spiral to the origin, the approach of solutions can be examined more carefully to exclude the lower

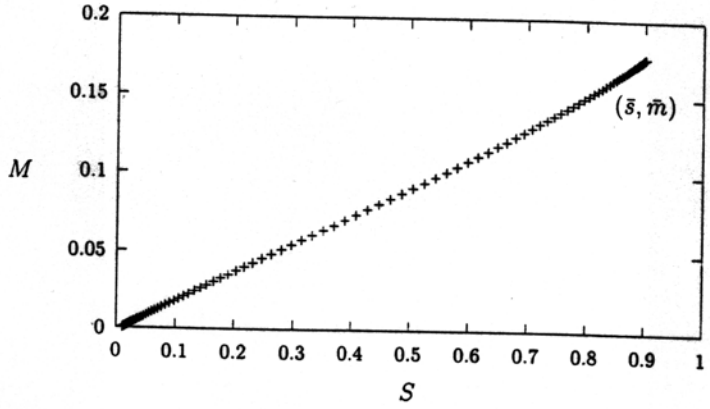

Fig. 4. Heteroclinic orbit to traveling wave problem (12), (14) with $c \in (c_2,\infty)$. The numerical solution, used a shooting method with a variable length of integration (see end of Section 4).

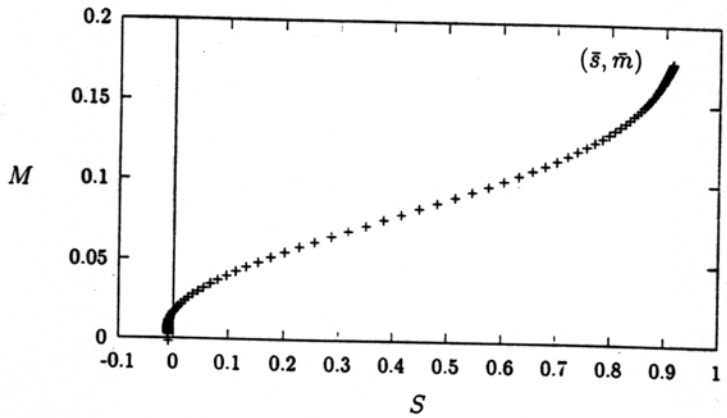

Fig. 5. Heteroclinic orbit to traveling wave problem (12), (14) with $c \in (c_1,c_2)$. The numerical solution, used a shooting method with a variable length of integration (see end of Section 4).

range. Orbits for the nonlinear system approach a stable node along the subspace spanned by the eigenvectors associated with negative eigenvalues of the system linearized about the node (BRAUN, 1983; GUCKENHEIMER and HOLMES, 1983). In Appendix A we show that for the lower range of possible wave speeds, $(0,c_1]$, both eigenvectors associated with negative eigenvalues of the node (0,0,0) have either a negative S or a negative M component, and thus trajectories violate our non-negativity assumption. Consequently, only wave speeds in the upper range $[c_2,\infty)$ are possible for this model.

We calculated the minimum wave speed c_2 numerically by fixing the value of μ and solving for the largest root of (24) as λ_{sm} and λ_{ms} were varied (Fig. 6). The surfaces in Fig.

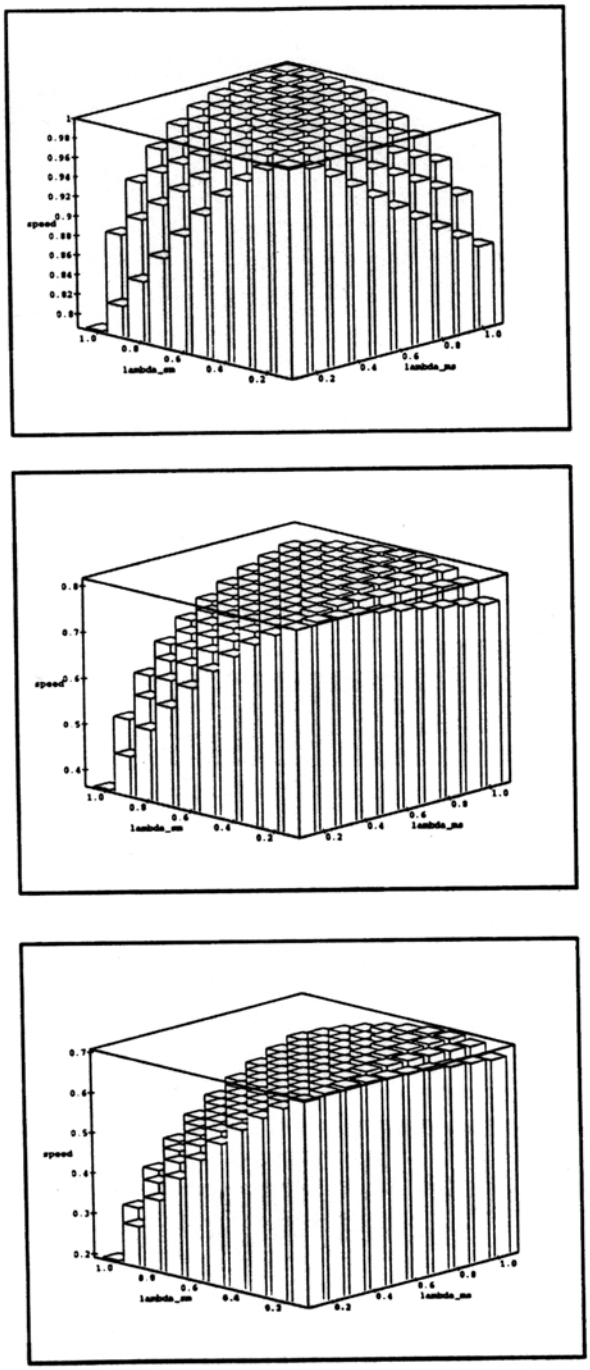

Fig. 6. Minimum wave speed c_2, calculated as the square root of the larger positive root of (32), and given as a function of transfer rates λ_{sm} and λ_{ms}. (a) Mortality rate $\mu = 0$. (b) Mortality rate $\mu = 0.5$. (c) Mortality rate $\mu = 1.0$.

6 illustrate a trade-off between benefits of growth plus no dispersal in the stationary class and mortality but dispersal in the mobile class. The balance required for the most rapid invasion is given by the high points on the surfaces in Fig. 6. Whereas the case $\mu=0$, shown in Fig. 6(a), indicates that invasion is fastest for equal transfer rates, the case $\mu>0$, shown in Figs. 6(b) and (c), indicates that invasion is fastest when λ_{ms} exceeds λ_{sm}.

We numerically investigated traveling wave solutions by solving the full system (1) via the method of lines and Gear's method for integration using a variety of different initial conditions. A domain size was chosen that was many times longer than the width of the wave. Boundary conditions were specified as being zero-flux. The wave speeds observed in the simulations are approximately equal to the minimum wave speed, c_2, calculated numerically from Eq. (24). Thus the numerical evidence indicates convergence of the initial data to a solution moving at the minimum wave speed. The convergence of related traveling waves has been analysed in depth for Fishers equation (BRAMSON, 1988).

6. Analysis of a Simplified Case

We consider here the case where there is no mortality in the mobile class and the transfer rates between mobile and stationary classes are identical

$$\mu = 0, \quad \lambda_{sm} = \lambda_{ms} = \lambda \tag{28}$$

(see Fig. 6). In this case, substitution into (24) yields the minimum wave speed as

$$c_2 = 1.$$

It is interesting to note that this is precisely half of the minimum wave speed for Fisher's equation, which describes simultaneous logistic growth and diffusive dispersal of a single population (MURRAY, 1989). We observe that the case with no mortality in the mobile class ($\mu = 0$), and equal transfer rates λ between mobile and stationary classes should equally distribute the fraction of time that an individual spends in the mobile and stationary classes and thus render an effective growth rate of $r = 1/2$ and diffusion coefficient $D = 1/2$. In this case our minimum wave speed of $c_2 = 1$ is consistent with the minimum wave speed for Fishers equation $2\sqrt{rD}$.

Perturbing the identical transfer rates by defining $\lambda_{ms} = \lambda_{sm} + \nu\varepsilon$, $\nu = \pm 1$, $0 \le \varepsilon \le \lambda_{sm}$, yields

$$R(1) = -\varepsilon^2\left(4\nu\varepsilon + 1 + 2\lambda_{sm} + \lambda_{sm}^2\right) \tag{29}$$

$$\le -\varepsilon^2\left(1 - \lambda_{sm}\right)^2, \tag{30}$$

(see (24)) thus indicating that $R(1) < 0$ for $\varepsilon \neq 0$. This, in turn, implies that $c_2 < 1$ for $\varepsilon \neq$

0 (Fig. 3) and thus the identical transfer rates yield the largest minimum wave speed. In the case where ε is a small parameter, the minimum wave speed c_2 can be calculated as a regularly perturbed series about $c_2 = 1$:

$$c_2 = 1 + \sum_i \gamma_i \varepsilon^i. \tag{31}$$

Substitution of $\lambda_{ms} = \lambda_{sm} + \varepsilon$ and $c = c_2$, as given above (31), into the cubic $R(c^2)$ (24), and grouping by successive orders of ε yields the coefficients γ_i, the first five of which are given in Appendix B. Note the fact that coefficients of the even powers of ε are negative is consistent with the above results regarding the maximum wave speed when $\varepsilon = 0$.

It is interesting to note that in the simplified case with no mortality and identical transfer rates (28) the minimum wave speed is independent of λ and is thus valid even as $\lambda \to 0$ and the two equations become uncoupled. The reason for this behavior can be found in the construction of an approximate solution.

Equation (8) is rewritten as

$$S' + S(1-S) - \lambda S + \lambda M = 0 \tag{32}$$

$$M' - \lambda S + \lambda M + M'' = 0, \tag{33}$$

and the boundary conditions remain as given by (9). Because the solution to the traveling wave problem is only unique modulo translation in the independent variable, we add the additional constraint $S(0) = 1/2$. This also centers the wave about the origin.

The system (32)–(33), (9) is singular for M; as $\lambda \to 0$, bounded solutions to (33) are constant and thus do not satisfy the boundary conditions (9). Using the compressed variable $\xi = \lambda z$ we rewrite (32)–(33) as

$$\lambda S_\xi + S(1-S) - \lambda S + \lambda M = 0 \tag{34}$$

$$\lambda M_\xi - \lambda S + \lambda M + \lambda^2 M_{\xi\xi} = 0. \tag{35}$$

Thus viewed on a large space scale of order ξ, (32)–(33) defines an "inner" transition layer for S, which can be matched with the "outer" solution defined by (34)–(35).

Thus to $\mathcal{O}(\lambda)$ we have the solution as

$$S = \left(1 + \exp(z)\right)^{-1}, \tag{36}$$

$$M = \begin{cases} 1 - \exp(\lambda z), & z < 0 \\ 0, & z \geq 0 \end{cases}. \tag{37}$$

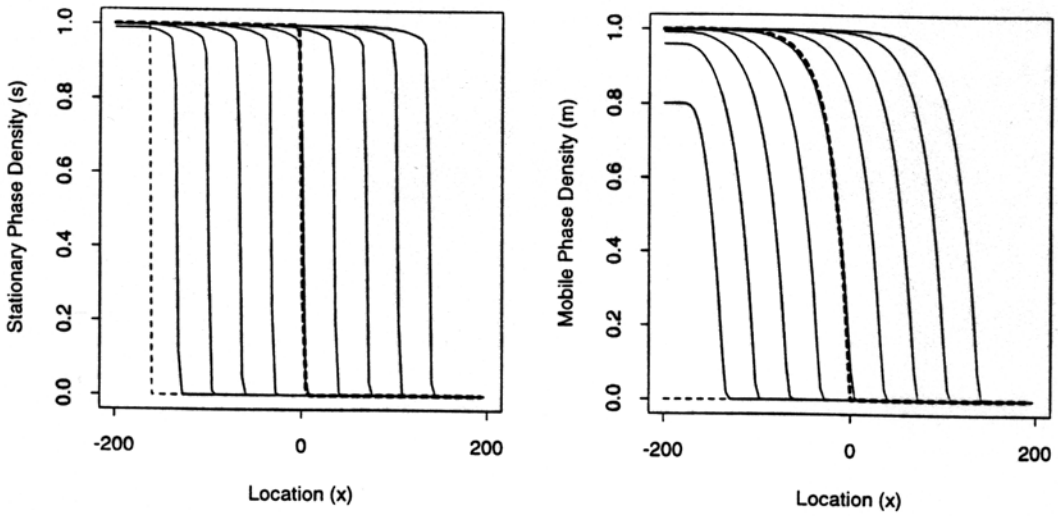

Fig. 7. Comparison of numerical solution of (4) and asymptotic solution (89)–(90) for $\mu = 0$ and $\lambda_{ms} = \lambda_{sm} = \lambda = 0.05$. Initial conditions for s are given by the light dashed line and initial conditions for m were identically zero. The solution for $t > 0$ is given by the solid line and is shown every 34 time units. The asymptotic solution, centered about $z = 0$, is given by the heavy dashed line. Boundary conditions are Neumann. The numerical solution method uses the Method of Lines and Gear's Method.

Figure 7 compares this approximate solution for the traveling wave to the numerically calculated solution. Notice that as $\lambda \to 0$ the first order approximate solution for S (36) remains unchanged. This describes a "kinematic" wave driven solely by the logistic reaction dynamics. The apparent movement of the wave is solely a function of the fact that each point in space lags slightly behind its neighbor to the left, and the shape of the wave is chosen precisely so as to give a constant speed. Whereas $\lambda > 0$ gives a minimum wave speed of $c = 1$, the $\lambda = 0$ case has no minimum wave speed associated with it. In other words, the O(1) equation associated with (32), $cS' + S(1 - S) = 0$, has a non-negative solution for all c.

7. Discussion

Our model is a first attempt to analyse invasion rates in the presence of individuals switching between distinct mobile and stationary classes. How fast the organisms invade is governed by a trade-off between reproduction in the stationary class and dispersal but mortality in the mobile class. This can be seen in Fig. 6, where the proportion of organisms in each of these two classes is governed by the switching rates λ_{sm} and λ_{ms}. Here the invasion is fastest if there is no mortality in the mobile class $\mu = 0$ and transfer rates between stationary and mobile classes are equal $\lambda_{sm} = \lambda_{ms}$. For this case the minimum speed of invasion, given in dimensional terms as $\sqrt{Dr}$, is exactly half that of Fisher's model ($2\sqrt{Dr}$), which describes a single population growing and dispersing (FISHER, 1937). Thus,

for populations switching between mobile and stationary states, Fisher's formula applied blindly to field measurements of the intrinsic growth rate and the mean squared displacement ($2Dt$) will overestimate spread rates to be more than twice their true value.

Our results also contrast with those of Cook (COOK, 1995) where it is assumed that individuals are born into either mobile or stationary subpopulations and remain there for life. For Cook's model,

$$\frac{\partial m}{\partial t} = D\frac{\partial^2 m}{\partial x^2} + \rho\phi(m+s)$$

$$\frac{\partial s}{\partial t} = (1-\rho)\phi(m+s),$$

where ϕ is the growth function, the minimum wave speed is calculated as $c = (1 + \sqrt{\rho})\sqrt{\phi'(0)D}$. Here $0 < \rho < 1$ describes the proportion of individuals born into the mobile population. This minimum wave speed for Cook's model is bounded above by that of Fisher's equation, and is bounded below by that of our model presented in this paper. The case $\mu = 0$ and $\lambda_{ms} = \lambda_{sm} = \lambda \to 0$ in our model has an analogy with the case $\rho \to 0$ with Cook's model. In both cases the mobile and stationary phases are only weakly coupled and the minimum wave speed approaches $\sqrt{D\phi'(0)}$. This warns ecologists that, even in the presence of an infinitesimally weak link between mobile and stationary classes, a population can invade at a significant rate.

In our analysis we consider only the case of motion by diffusion. The mobile class could possibly move by a mixture of diffusion and convection. While our analysis could be simply extended to cover this case, numerical simulations show the addition of a convective term corresponding to bulk flow in the mobile class can serve to slow down or even reverse an invasion.

Many thanks to Julian Cook, Peter Kareiva and Jim Murray for valuable discussions. This work was supported in part from a grant from the Environmental Protection Agency, by NSF grant DMS-9457816 and by an Alfred P. Sloan research fellowship.

APPENDIX A

Excluding the Lower Range

To show orbits are negative for the range of wave speeds $(0, c_1)$, we find an expression $\phi(c, \sigma_i(c))$ relating the S and M components of the eigenvectors and derive a differential equation involving this expression. Solving this differential equation yields an expression that allows us to evaluate the sign of $\phi(c, \sigma_i(c))$. For wave speeds in $(0, c_1)$ the sign is negative and for wave speeds in (c_2, ∞) the sign is positive. That is, given eigenvalues for J (41)

evaluated at (0,0,0) $\sigma_1 < \sigma_2 < 0$ and associated eigenvectors $\boldsymbol{v}_i = (v_{i1}, v_{i2}, v_{i3})^T$, $i = 1, 2$, we will show that $c \in (0, c_1)$ implies

$$\operatorname{sgn}(v_{i1}) \neq \operatorname{sgn}(v_{i2}), \quad i = 1, 2, \tag{38}$$

and that $c \in (c_2, \infty)$ implies

$$\operatorname{sgn}(v_{i1}) = \operatorname{sgn}(v_{i2}), \quad i = 1, 2. \tag{39}$$

By definition, σ_i, and $\boldsymbol{v}_i$, $i = 1, 2$, satisfy

$$(J - \sigma_i I)\boldsymbol{v}_i = 0, \tag{40}$$

where the linearized matrix associated with (8) is:

$$J = \begin{bmatrix} -\frac{1}{c}\left(-2S + (1 - \lambda_{sm})\right) & \frac{-\lambda_{ms}}{c} & 0 \\ 0 & 0 & 1 \\ -\lambda_{sm} & \mu + \lambda_{ms} & -c \end{bmatrix}. \tag{41}$$

Solving this system of equations we find that

$$\left(-\frac{k_2}{c} - \sigma_i\right) v_{i1} - \frac{\lambda_{ms}}{c} v_{i2} = 0 \tag{42}$$

or

$$v_{i2} = \phi(c, \sigma_i(c)) v_{i1} \tag{43}$$

where

$$\phi(c, \sigma_i(c)) = -\frac{1}{\lambda_{ms}}(k_2 + c\sigma_i(c)). \tag{44}$$

Notice that ϕ depends both on c and σ_i, and that the eigenvalue σ_i also depends on c. The sign of $\phi(c, \sigma_i(c))$ depends on the relative sizes of the eigenvalue, σ_i and k_2. As written, evaluation of $\operatorname{sgn}(\phi(c, \sigma_i(c)))$ is inconclusive. In order to determine the sign, we derive a

differential equation. We do so by first differentiating $\phi(c,\sigma_i(c))$:

$$\frac{d\phi\left(c,\sigma_i(c)\right)}{dc} = -\frac{1}{\lambda_{ms}}\left(c\frac{d\sigma_i(c)}{dc} + \sigma_i(c)\right). \tag{45}$$

To evaluate this derivative, we need $d\sigma_i(c)/dc$. To calculate $d\sigma_i(c)/dc$, we consider P_0 evaluated at the eigenvalue σ_i and differentiate implicitly:

$$\frac{\partial}{\partial c}\left(P_0\left(\sigma_i\right)\right) = \frac{\partial}{\partial c}\left(\sigma_i^3 + A_1\sigma_i^2 + A_2\sigma_i + A_3\right). \tag{46}$$

Because $P_0(\sigma_i(c))$ is identically zero for all c, so is $\partial P_0(\sigma_i(c))/dc$. Thus,

$$\frac{\partial P_0\left(\sigma_i(c)\right)}{\partial \sigma_i}\frac{d\sigma_i(c)}{dc} + \frac{\partial P_0\left(\sigma_i(c)\right)}{\partial A_1}\frac{dA_1}{dc} + \frac{\partial P_0\left(\sigma_i(c)\right)}{\partial A_3}\frac{dA_3}{dc} = 0. \tag{47}$$

Solving for $d\sigma_i(c)/dc$ we have

$$\frac{d\sigma_i(c)}{dc} = -\frac{\sigma_i^2\frac{dA_1}{dc} + \frac{dA_3}{dc}}{3\sigma_i^2 + 2A_1\sigma_i + A_2}. \tag{48}$$

Using the fact that

$$c\frac{dA_3}{dc} = -A_3 \tag{49}$$

and

$$A_1 - c\frac{dA_1}{dc} = 2\frac{k_2}{c}, \tag{50}$$

we have

$$\frac{d\phi\left(c,\sigma_i(c)\right)}{dc} = -\frac{1}{\lambda_{ms}}\left(\frac{3\sigma_i^3 + \left(A_1 + 2\frac{k_2}{c}\right)\sigma_i^2 + A_2\sigma_i + A_3}{3\sigma_i^2 + 2A_1\sigma_i + A_2}\right). \tag{51}$$

Adding $-P_0(\sigma_i)$, which is identically zero, we have

$$\frac{d\phi(c,\sigma_i(c))}{dc} = -\frac{1}{\lambda_{ms}}\left(\frac{2\sigma_i^2(k_2+c\sigma_i)}{c(3\sigma_i^2+2A_1\sigma_i+A_2)}\right). \tag{52}$$

This is a first order linear differential equation; namely,

$$\frac{d\phi(c,\sigma_i(c))}{dc} = h(c,\sigma_i(c))\phi(c,\sigma_i(c)) \tag{53}$$

where

$$h(c,\sigma_i(c)) = \frac{2\sigma_i^2}{c(3\sigma_i^2+2A_1\sigma_i+A_2)}. \tag{54}$$

The solution of this equation is an expression for $\phi(c,\sigma_i(c))$ of which we can evaluate the sign.

Notice that the denominator of $h(c,\sigma_i(c))$ is precisely the derivative of P_0 with respect to σ evaluated at σ_i. Thus for c in the intervals $(0,c_1)$ and (c_2,∞) the denominator is positive at σ_1 and negative at σ_2 (see Fig. 2(a)) so that

$$h(c,\sigma_1(c)) > 0 \tag{55}$$

$$h(c,\sigma_2(c)) < 0. \tag{56}$$

Note that $h(c,\sigma_i(c))$ is undefined when $c = c_1$ or $c = c_2$ (see Fig. 2(b)). We now consider two cases: $0 < c \le c_1$ and $c_2 \le c < \infty$.

Case I: $c \in (0,c_1]$

By solving the differential Eq. (53) with two different initial conditions, we show that in this range, v_{i1} and v_{i2} have opposite signs, or in other words

$$\phi(c,\sigma_i(c)) < 0 \tag{57}$$

see (43).

To find an initial condition, we investigate how the two negative roots of P_0, (11), σ_1 and σ_2 behave as $c \to 0$. An asymptotic expansion in powers of c yields

$$\sigma_1 = -\frac{k_2}{c} + \frac{\lambda_{sm}\lambda_{ms}}{k_2^2}c + \mathbb{O}\left(c^2\right) \tag{58}$$

and

$$\sigma_2 = -\sqrt{\frac{\lambda_{sm}\lambda_{ms} + k_1 k_2}{k_2}} + \mathbb{O}(c). \tag{59}$$

Using (53) and $i = 1$ we have a differential equation for $\phi(c,\sigma_1(c))$, the expression relating the first and second components of ν_1 (see (43)). Choosing $0 < c_\varepsilon << 1$ and substituting in (44) we have

$$\begin{aligned}\phi_{11}(c_\varepsilon) &= \phi\left(c_\varepsilon, \sigma_1(c_\varepsilon)\right) \\ &= \frac{-\lambda_{sm}}{k_2^2}c_\varepsilon^2 + \mathbb{O}\left(c_\varepsilon^3\right) \\ &< 0,\end{aligned} \tag{60}$$

which serves as an initial condition for the differential equation

$$\frac{d\phi\left(c,\sigma_1(c)\right)}{dc} = h\left(c,\sigma_1(c)\right)\phi\left(c,\sigma_1(c)\right). \tag{61}$$

The unique solution to the equation with initial condition (60) is

$$\phi\left(c,\sigma_1(c);c_\varepsilon\right) = \phi_{11}(c_\varepsilon)\exp\left(\int_{c_\varepsilon}^{c} h\left(\gamma,\sigma_1(\gamma)\right)d\gamma\right), \tag{62}$$

for $c \in (c_\varepsilon, c_1)$. Thus, because $\phi_{11}(c_\varepsilon) < 0$ we have

$$\phi\left(c,\sigma_1(c)\right) < 0 \tag{63}$$

for all $c \in (c_\varepsilon, c_1)$. Furthermore, this result holds for c_ε arbitrarily small, so (63) is true for $c \in (0, c_1)$.

The same conclusion holds for σ_2. Choosing c_ε sufficiently small we have the following initial condition:

$$\phi_{12}(c_\varepsilon) = \phi\left(c_\varepsilon, \sigma_2(c_\varepsilon)\right) = -\frac{k_2}{\lambda_{ms}} + \mathcal{O}(c). \tag{64}$$

Solving

$$\frac{d\phi\left(c, \sigma_2(c)\right)}{dc} = h\left(c, \sigma_2(c)\right)\phi\left(c, \sigma_2(c)\right) \tag{65}$$

for (64), we have

$$\phi\left(c, \sigma_2(c); c_\varepsilon\right) = \phi_{12}(c_\varepsilon)\exp\left(\int_{c_\varepsilon}^{c} h\left(\gamma, \sigma_2(\gamma)\right)d\gamma\right) \tag{66}$$

for $c \in (c_\varepsilon, c_1)$. Thus, because $\phi_{12}(c_\varepsilon) < 0$, we have

$$\phi\left(c, \sigma_2(c)\right) < 0 \tag{67}$$

for all $c \in (c_\varepsilon, c_1)$. Furthermore, this result holds for c_ε arbitrarily small, so (67) is true for $c \in (0, c_1)$.

It is interesting to look at $d\phi(c, \sigma_i(c))/dc$ as well. Using (55) and (63) we observe that

$$\frac{d\phi\left(c, \sigma_1(c)\right)}{dc} = h\left(c, \sigma_1(c)\right)\phi\left(c, \sigma_1(c)\right) < 0. \tag{68}$$

That is, the slope of the v_1 eigenvector in the *S*-*M* plane gets more negative as c increases. Using (56) and (67) we observe that

$$\frac{d\phi\left(c, \sigma_2(c)\right)}{dc} = h(c)\phi\left(c, \sigma_2(c)\right) > 0. \tag{69}$$

That is, the slope of the v_2 eigenvector in the *S*-*M* plane is getting less negative as c increases. As $c \to c_1$, the eigenvectors approach one another, as in Fig. 8. This result can also be verified numerically for test parameters. Numerically, as $c \to c_1$, both the eigenvalues and the eigenvectors approach each other.

By solving Eq. (53) for different initial conditions, we have shown that $\phi(c, \sigma_i(c)) < 0$ for $c \in (0, c_1)$. Thus, the *S* and *M* components of eigenvectors v_1 and v_2 have opposite

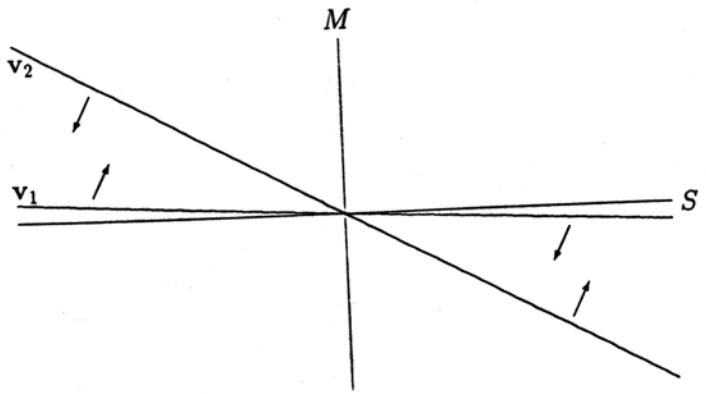

Fig. 8. Behavior of the eigenvectors (40)–(41) as c increases to c_1.

signs, and as an orbit approaches along either eigenvector, one of S and M will be negative. Because these quantities must both be non-negative by assumption, we exclude the range of wave speeds $(0,c_1)$. Continuous dependence of the eigenvectors to (41) on the wave speed c means that this interval of exclusion can be extended to $(0,c_1]$.

Case II: $c \in [c_2,\infty)$

Having shown that $\phi(c,\sigma_i(c)) < 0$ in the interval $(0,c_1)$, and thus having excluded this interval as not satisfying the non-negativity assumption, we now to show that non-negativity can be obeyed for wave speeds in $[c_2,\infty)$. We start by showing that for $c \in (c_2,\infty)$

$$\phi\left(c,\sigma_i(c)\right) > 0, \tag{70}$$

and thus substitution into (43) shows that (39) is satisfied.

Again, we expand σ_i asymptotically. For $c >> 0$,

$$\sigma_1 = -c + \mathcal{O}(1) \tag{71}$$

and

$$\sigma_2 = \frac{1}{2c}\left[\left(k_1 - k_2\right) - \sqrt{\left(k_2 + k_1\right)^2 + 4\lambda_{sm}\lambda_{ms}}\right] + \mathcal{O}\left(1/c^2\right). \tag{72}$$

We find a differential equation for $\phi(c,\sigma_2(c))$. We choose large c_ε such that $0 < 1/c_\varepsilon << 1$. The initial condition is found by substituting c_ε in (44):

$$\begin{aligned}\phi_{22}(c_\varepsilon) &= \phi\left(c_\varepsilon, \sigma_2(c_\varepsilon)\right) \\ &= -\frac{1}{2\lambda_{ms}}\left(k_1 + k_2 - \sqrt{(k_1+k_2)^2 + 4\lambda_{sm}\lambda_{ms}}\right) \\ &> 0. \end{aligned} \tag{73}$$

Solving

$$\frac{d\phi(c, \sigma_2(c))}{dc} = h(c, \sigma_2(c))\phi(c, \sigma_2(c)) \tag{74}$$

with condition (73), we have

$$\begin{aligned}\phi(c, \sigma_2(c); c_\varepsilon) &= \phi_{22}(c_\varepsilon)\exp\left(\int_{c_\varepsilon}^{c} h(\gamma, \sigma_1(\gamma))d\gamma\right) \\ &= \phi_{22}(c_\varepsilon)\exp\left(\int_{c}^{c_\varepsilon} -h(\gamma, \sigma_1(\gamma))d\gamma\right)\end{aligned} \tag{75}$$

for $c \in (c_2, c_\varepsilon)$. Thus, because $\phi_{22}(c_\varepsilon) > 0$ we have

$$\phi(c, \sigma_1(c)) > 0 \tag{76}$$

for all $c \in (c_2, c_\varepsilon)$. Furthermore, this result holds for $1/c_\varepsilon$ arbitrarily small, so (76) is true for $c \in (c_2, \infty)$.

Finally we consider σ_1 for c in (c_2, ∞). We use the same procedure as previously, but in order to avoid problems in taking limits, we solve a slightly different differential equation. We find a differential in the inverse function of $\phi(c, \sigma_1(c))$, and solve, given an initial condition. We use the inverse so that our initial condition approaches 0 rather than ∞ as $c \to \infty$. Consider instead the function $(\phi(c, \sigma_1(c)))^{-1}$. Differentiating we have

$$\begin{aligned}\frac{d\left(\phi(c, \sigma_1(c))\right)^{-1}}{dc} &= -\frac{1}{\left(\phi(c, \sigma_1(c))\right)^2}\frac{d\phi(c, \sigma_1(c))}{dc} \\ &= -\frac{1}{\left(\phi(c, \sigma_1(c))\right)^2}\left(\frac{2\sigma_1^2}{c\left(3\sigma_1^2 + 2A_1\sigma_1 + A_2\right)}\right)\phi(c, \sigma_1(c)) \\ &= -h(c, \sigma_1(c))\left(\phi(c, \sigma_1(c))\right)^{-1}.\end{aligned} \tag{77}$$

Choosing $c_\varepsilon >> 0$ and then substituting, we have the initial condition

$$\begin{aligned}\left(\phi_{21}(c_\varepsilon)\right)^{-1} &= \left(\phi\left(c_\varepsilon, \sigma_1(c_\varepsilon)\right)\right)^{-1} \\ &= -\frac{\lambda_{ms}}{k_2 - c_\varepsilon^2} > 0. \end{aligned} \tag{78}$$

Solving (77) with condition (78), we have

$$\left(\phi\left(c, \sigma_1(c), c_\varepsilon\right)\right)^{-1} = \left(\phi_{21}(c_\varepsilon)\right)^{-1} \exp\left(\int_{c_\varepsilon}^{c} -h\left(\gamma, \sigma_1(\gamma)\right) d\gamma\right) \tag{79}$$

for $c \in (c_2, c_\varepsilon)$. Thus, because $(\phi_{21}(c_\varepsilon))^{-1} > 0$ we have

$$\left(\phi\left(c, \sigma_1(c)\right)\right)^{-1} > 0, \tag{80}$$

which implies that

$$\phi\left(c, \sigma_1(c)\right) > 0. \tag{81}$$

Initial condition (78) is bounded for c_ε arbitrarily large, so the result holds for c_ε arbitrarily large, and we conclude that (81) is valid on (c_2, ∞).

Again it is interesting to examine how the eigenvectors change with c. Using (55) and (81) we observe that

$$\frac{d\phi\left(c, \sigma_1(c)\right)}{dc} = h\left(c, \sigma_1(c)\right)\phi\left(c, \sigma_1(c)\right) > 0. \tag{82}$$

That is, the slope of the $\boldsymbol{v}_1$ eigenvector in the *S-M* plane decreases as c decreases from ∞. Using (56) and (81) we observe that

$$\frac{d\phi\left(c, \sigma_2(c)\right)}{dc} = h\left(c, \sigma_2(c)\right)\phi\left(c, \sigma_2(c)\right) < 0. \tag{83}$$

That is, the slope of the $\boldsymbol{v}_2$ eigenvector in the *S-M* plane increases as c decreases from ∞. As $c \to c_2^+$, the eigenvectors approach each another as shown in Fig. 9. Continuous dependence of the eigenvectors to (41) on the wave speed c means that non-negativity of solutions can be extended from the interval (c_2, ∞) to $[c_2, \infty)$.

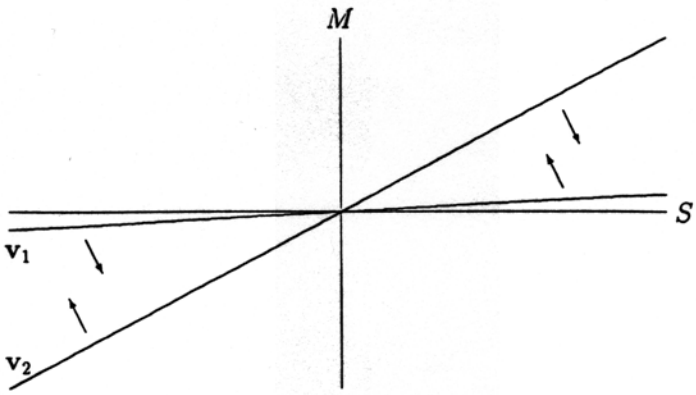

Fig. 9. Behavior of the eigenvectors (40)–(41) as c decreases to c_2.

We thus summarize the results proven above as follows: If $\sigma_1 < \sigma_2 < 0$ are eigenvalues for the Jacobian matrix J (41), with associated eigenvectors $v_i = (v_{i1}, v_{i2}, v_{i3})^T$, then for $\phi(c,\sigma_i(c)) = -(1/\lambda_{ms})(k_2 + c\sigma_i)$, $v_{i2} = \phi(c,\sigma_i(c))v_{i1}$. Further, if c_1 and c_2 exist, then for $c \in (0,c_1)$, $\phi(c,\sigma_i(c)) < 0$, and for $c \in (c_2,\infty)$, $\phi(c,\sigma_i(c)) > 0$. Therefore orbits associated with solutions having wave speeds in the range $(0,c_1)$ must be negative in S or M as they approach the origin because the S and M components of the eigenvectors v_1 and v_2 have opposite signs. These solutions are not meaningful biologically and violate our requirement of non-negativity. Orbits with wave speeds in (c_2,∞) are allowed, as they approach the origin along eigenvectors whose S and M components can have the same sign. Continuity arguments can be used to extend the above intervals so that solutions must be negative for $c \in (0,c_1]$ and can be non-negative for $c \in [c_2,\infty)$. Thus, only waves with speeds in $[c_2,\infty)$ are biologically plausible and can be non-negative.

APPENDIX B

Asymptotic Expansion for c_2

Substitution of (31) into (24), and evaluation of the σ_is for successive orders of ε yields:

$$\gamma_1 = 0,$$

$$\gamma_2 = -\frac{1}{(4\lambda_{ms} + 4)\lambda_{ms}},$$

$$\gamma_3 = \frac{2\lambda_{ms}^2 + 2\lambda_{ms} + 1}{8\lambda_{ms}^2\left(\lambda_{ms}^3 + 3\lambda_{ms} + 1 + 3\lambda_{ms}^2\right)},$$

$$\gamma_4 = -\frac{12\lambda_{ms}^4 + 20\lambda_{ms}^3 + 32\lambda_{ms}^2 + 20\lambda_{ms} + 5}{64\lambda_{ms}^3\left(\lambda_{ms}^5 + 5\lambda_{ms}^4 + 10\lambda_{ms}^3 + 10\lambda_{ms}^2 + 5\lambda_{ms} + 1\right)},$$

$$\gamma_5 = \frac{16\lambda_{ms}^6 + 32\lambda_{ms}^5 + 116\lambda_{ms}^4 + 144\lambda_{ms}^3 + 106\lambda_{ms}^2 + 42\lambda_{ms} + 7}{128\lambda_{ms}^4\left(\lambda_{ms}^7 + 7\lambda_{ms}^6 + 21\lambda_{ms}^5 + 35\lambda_{ms}^4 + 35\lambda_{ms}^3 + 21\lambda_{ms}^2 + 7\lambda_{ms} + 1\right)}.$$

REFERENCES

AMANN, H. (1990) *Ordinary Differential Equations*, de Gruyter, Berlin.

BRAMSON, M. (1988) Convergence to traveling waves for systems of Kolmogorov-like parabolic equations, in *Nonlinear Diffusion Equations and Their Equilibrium States* (eds. W. M. Ni, L. A. Peletier and J. Serrin), Springer-Verlag, New York/Berlin, pp. 179–190.

BRAUN, M. (1983) *Differential Equations and Their Applications, Volume 15 of Applied Mathematical Sciences*, Springer-Verlag, New York.

COOK, J. (1995) Dispersive variability and invasion wave speeds. Submitted Manuscript.

FISHER, R. A. (1937) The wave of advance of advantageous genes, *Ann. of Eugenics*, **7**, 355–369.

FRIEDMAN, M. J. and DOEDEL, E. J. (1991, June) Numerical computation and continuation of invariant manifolds connecting fixed points, *SIAM J. Numer. Anal.* **28**(3), 789–808.

GUCKENHEIMER, J. and HOLMES, P. (1983) *Nonlinear Oscillations, Dynamical Systems and Bifurcations of Vector Fields, Volume 42 of Applied Mathematical Sciences*, Springer-Verlag, New York.

KOT, M. (1992) Discrete-time travelling waves: Ecological examples, *J. Math. Biol.*, **30**, 413–436.

LEWIS, M. A., KAREIVA, P. and TREVORS, J. T. (1995) Models to examine containment and spread of genetically engineered microbes, *Microbial Ecology* (in press).

MURRAY, J. D. (1989) *Mathematical Biology, Volume 19 of Biomathematics*, Springer-Verlag, New York.

SCHMITZ, G. (1993) A model for the spread of genetically engineered microbes. Master's Thesis, University of Utah.

VEIT, R. and LEWIS, M. A. (1995) Dispersal, population growth and the Allee effect: Dynamics of the house finch invasion of eastern north America, *American Naturalist* (in press).